

Changes in biomass burning, wetland extent, or agriculture drive atmospheric NH₃ trends in several African regions

Jonathan E. Hickman^{1*}, Niels Andela^{2†}, Enrico Dammers³, Lieven Clarisse⁴, Pierre-François Coheur⁴, Martin Van Damme⁴, Courtney Di Vittorio⁵, Money Ossohou⁶, Corinne Galy-Lacaux⁷, Kostas Tsigirdis^{1,8}, Susanne Bauer¹

¹NASA Goddard Institute for Space Studies, New York, USA

²NASA Goddard Space Flight Center, Beltsville, USA

³Air Quality Research Division, Environment and Climate Change Canada, Toronto, Canada

⁴Université libre de Bruxelles (ULB), Service de Chimie Quantique et Photophysique, Atmospheric Spectroscopy, Brussels, Belgium

⁵Wake Forest University, Winston-Salem, USA

⁶~~Laboratoire des Sciences de la Matière, de l'Environnement et de l'Energie Solaire,~~ Université Félix Houphouët-Boigny, Abidjan, Côte d'Ivoire

⁷Laboratoire d'Aérodynamique, Université Toulouse III Paul Sabatier / CNRS, France

⁸Columbia University, New York, USA

[†]Now at School of Earth and Ocean Sciences, Cardiff University, Cardiff, UK

*Correspondence to: jonathan.e.hickman@nasa.gov

Abstract

Atmospheric ammonia (NH₃) is a precursor to fine particulate matter and a source of nitrogen (N) deposition that can adversely affect ecosystem health. The main sources of NH₃—agriculture and biomass burning—are undergoing or expected to undergo substantial changes in Africa. Although evidence of increasing NH₃ over parts of Africa has been observed, the mechanisms behind these trends are not well understood. Here we use

Deleted: Laboratoire de Physique de l'Atmosphère et de Mécanique des Fluides

33 observations of atmospheric NH₃ vertical column densities (VCDs) from the Infrared
 34 Atmospheric Sounding Interferometer (IASI) along with other satellite observations of the
 35 land surface and atmosphere to evaluate how NH₃ concentrations have changed over Africa
 36 from 2008 through 2018, and what has caused those changes. In West Africa NH₃ VCDs are
 37 observed to increase during the late dry season, with increases of over 7% yr⁻¹ in Nigeria
 38 during February and March ($p < 0.01$). These positive trends are associated with increasing
 39 burned area and CO trends during these months, likely related to agricultural preparation.
 40 Increases are also observed in the Lake Victoria Basin, where they are associated with
 41 expanding agricultural area. In contrast, NH₃ VCDs declined over the Sudd wetlands in
 42 South Sudan by over 2% yr⁻¹ ($p = 0.20$). Annual maxima in NH₃ VCDs in South Sudan occur
 43 during February through May and are associated with drying of temporarily flooded
 44 wetland soils, which favor emissions of NH₃. The change in mean NH₃ VCDs over the Sudd
 45 is strongly correlated with variation in wetland extent in the Sudd: in years when more
 46 area remained flooded during the dry season, NH₃ concentrations were higher ($r = 0.65$,
 47 $p = 0.04$). Relationships between biomass burning and NH₃ may be observed when
 48 evaluating national-scale statistics: countries with the highest rates of increasing NH₃ VCDs
 49 also had high rates of growth in CO VCDs; burned area displayed a similar pattern, though
 50 not significantly. Livestock numbers were also higher in countries with intermediate or
 51 high rates of NH₃ VCD growth. Fertilizer use in Africa is currently low but growing;
 52 implementing practices that can limit NH₃ losses from fertilizer as agriculture is intensified
 53 may help mitigate impacts on health and ecosystems.

1. Introduction:

57 Ammonia (NH₃), a reactive nitrogen (N) trace gas, plays a number of important roles
 58 in the atmosphere, with implications for human health, climate, and ecosystems. Once in
 59 the atmosphere, NH₃ contributes to the production of inorganic aerosols, the primary
 60 constituents of fine particulate matter and a serious health hazard (Bauer et al., 2016;
 61 Lelieveld et al., 2015; Pope et al., 2002). NH₃ can also be deposited to downwind
 62 ecosystems, contributing to eutrophication, soil acidification, vegetation damage,
 63 productivity declines, reductions in biodiversity, and indirect greenhouse gas emissions

Deleted: 7

Deleted: We find that NH₃ VCDs have increased over several regions, including much of West Africa and parts of the Lake Victoria Basin.

Deleted: 6

Deleted: South Sudan

Deleted: during the February through May period, with the largest rates of change over the Sudd wetlands

Deleted: and all of South Sudan during February through May ...

Deleted: 9

Deleted: 3

Deleted: agriculture

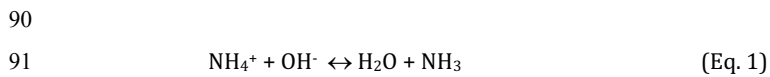
Deleted: can

Deleted: the largest declines in NH₃ VCDs

Deleted: concentrations over time tended to have the smallest growth rates in crop productivity and livestock numbers as well as smaller negative changes in burned area than other countries.

83 (Denier Van Der Gon and Bleeker, 2005; Krupa, 2003; Matson et al., 1999; Stevens et al.,
84 2018; Tian and Niu, 2015).

85 Although NH_3 is emitted from natural soils, agriculture is by far the largest source of
86 NH_3 globally (Behera et al., 2013; Bouwman et al., 1997). Urea fertilizer and livestock
87 excreta are particularly important substrates for NH_3 formation, and can be volatilized
88 quickly under favorable environmental conditions (Bouwman et al., 1997). In all soils, NH_3
89 is formed in solution following the dissociation of ammonium (NH_4^+ ; Eq. 1).



93 Soil NH_3 production is temperature-dependent, doubling with every 5°C temperature
94 increase, though the actual soil NH_3 flux is determined in part by plant and soil physiological
95 and physical factors (Sutton et al., 2013). On average, fertilizer use has been extremely low
96 in sub-Saharan Africa—often an order of magnitude or more lower than typical in Europe,
97 the United States, or China (Hazell and Wood, 2008; Vitousek et al., 2009). Livestock manure
98 N content also tends to be very low in sub-Saharan Africa (Rufino et al., 2006); the low
99 fertilizer use suggests that natural soils (as opposed to agricultural soils) may be a more
100 important source in the region than elsewhere in the world. However, agricultural
101 intensification and increasing fertilizer use has been a central policy focus for many African
102 countries, with national and regional efforts to increase N inputs by an order of magnitude
103 or more (AGRA, 2009).

104 After agriculture, biomass burning is the most important source of NH_3 globally
105 (Bouwman et al., 1997), with roughly 60 to 70% of global NH_3 emissions from fires occurring
106 in Africa (Cahoon et al., 1992; Whitburn et al., 2015). The amount of NH_3 emitted from
107 biomass fires is controlled primarily by the type of burning that occurs. N in fuel is present
108 predominantly in a chemically reduced state, and NH_3 is emitted in greater quantities from
109 low temperature, smoldering combustion in which fuel N is incompletely oxidized (Goode et
110 al., 1999; Yokelson et al., 2008). Fuel moisture content, which can help determine whether
111 combustion is smoldering or flaming, is thus an important determinant of biomass burning
112 NH_3 emissions (Chen et al., 2010).

Deleted: manure quality and

114 In contrast to other reactive N gases such as NO_x (nitric oxide + nitrogen dioxide),
115 NH₃ emissions are typically unregulated outside of Europe (Anker et al., 2018; Kanter,
116 2018; USDA Agricultural Air Quality Task Force, 2014), and substantial increasing trends
117 have been observed by the NASA Atmospheric InfraRed Sounder (AIRS) and the Infrared
118 Atmospheric Sounding Interferometer (IASI), over many of the world's major agricultural
119 and biomass burning regions during the 21st century (Van Damme et al., 2021; Warner et
120 al., 2017). West Africa has been identified as an important NH₃ source region (Van Damme
121 et al., 2018), where a trend of increasing NH₃ concentrations over 2002 to 2013 has been
122 attributed at least in part to increased fertilizer use (Van Damme et al., 2021; Warner et al.,
123 2017). Increasing trends have also been observed over central Africa, and attributed to
124 higher rates of biomass burning (Van Damme et al., 2021; Warner et al., 2017). However,
125 the studies by Warner et al. (2017) and Van Damme et al. (2021) were global in nature,
126 and as such could not include detailed explorations of the drivers of trends such as
127 consideration of emission seasonality or the geographic distribution of emission drivers,
128 which are particularly important across large parts of Africa where both biomass burning
129 and soils are potentially important sources (van der A et al., 2008).

130 Here we use a ten-year satellite record to evaluate trends in atmospheric NH₃
131 concentrations over Africa from 2008 through 2017, including detailed examination of
132 three regions where changes are pronounced: West Africa, the Lake Victoria Region, and
133 South Sudan.

135 2. Data and Methods

136 2.1 Global gridded data

137 Multiple data products were used, including satellite observations and spatial
138 datasets:

139 IASI-A, launched aboard the European Space Agency's MetOp-A in 2006, provides
140 measurements of atmospheric NH₃ and carbon monoxide (CO) twice a day (9:30 in the
141 morning and evening, Local Solar Time at the equator). Here we use morning observations,
142 when the thermal contrast is more favorable for retrievals (Clarisse et al., 2009; Van
143 Damme et al., 2014a). The NH₃ retrieval product used (ANNI-NH₃-v3R) follows a neural
144 network retrieval approach. We refer to Van Damme et al. (2017) and Van Damme et al.

Deleted:

Deleted: y

Deleted: as

Deleted: The Infrared Atmospheric Sounding Interferometer (...)

Deleted:)

Deleted: 2.2

152 [\(2021\)](#) for a detailed description of the algorithm. For CO, we used the product obtained
 153 with the FORLI v20140922 retrieval algorithm (Hurtmans et al., 2012). Given the absence
 154 of hourly or even daily observations of NH₃ concentrations in sub-Saharan Africa, the
 155 detection limit of IASI is difficult to determine with certainty. However, the region
 156 experiences high thermal contrast, and IASI seems to be able to reliably observe NH₃ down
 157 to 1 to 2 ppb at the surface (Clarisse et al., 2009; Van Damme et al., 2014b). We gridded the
 158 Level-2 IASI NH₃ and CO products to 0.25° × 0.25° resolution to match the resolution of
 159 other data used in the analysis. [We used a conventional binning approach based on the](#)
 160 [center of each satellite footprint. We did not apply an averaging weight. Quality control](#)
 161 [procedures were followed as detailed in van Damme et al. 2017 and Van Damme et al.](#)
 162 [2021. Specifically, the screening of retrievals included filtering of retrievals where cloud](#)
 163 [cover is over 10%, where the total column density is below zero and the absolute value of](#)
 164 [the hyperspectral range index \(HRI\) is above 1.5, and where the ratio of the total column](#)
 165 [density to HRI is larger than 1.5 × 10¹⁶ molecules cm⁻².](#)

Deleted: Only observations with cloud cover below 20% were used. ...

Deleted: re

166 The IASI products [s have](#) been validated using ground-based Fourier transform
 167 infrared (FTIR) observations of NH₃ total columns, with robust correlations at sites with
 168 high NH₃ concentrations, but lower at sites where atmospheric concentrations approach
 169 IASI's detection limits (Dammers et al., 2016; Guo et al., 2021). Compared to the FTIR
 170 observations, total columns from previous IASI NH₃ products (IASI-LUT and IASI-NNv1)
 171 are biased low by ~30% which varies per region depending on the local concentrations.
 172 [Although FTIR observations are absent from Africa, earlier work has shown fair agreement](#)
 173 [between previous versions of IASI total column densities and surface observations of NH₃](#)
 174 [using passive samplers across the International Network to study Deposition and](#)
 175 [Atmospheric chemistry in AFrica \(INDAAF\) network in West Africa](#) (Van Damme et al.,
 176 2015). [including in observations of seasonal variation](#) (Hickman et al., 2018; Ossohou et al.,
 177 2019). Validation of the IASI CO product using surface, aircraft, and satellite observations
 178 have found total columns to have an error that is generally below 10-15% in the tropics
 179 and mid-latitudes (George et al., 2009; Kerzenmacher et al., 2012; Pommier et al., 2010; De
 180 Wachter et al., 2012). The IASI NH₃ and CO products were used for the years 2008—the
 181 first full year of data available—to the end of 2018. [Random errors in observations can be](#)

Deleted: has

Field Code Changed

Deleted: IASI performed well in comparisons with surface observations of NH₃ concentrations in west and central Africa (Hickman et al., 2018; Ossohou et al., 2019)

Deleted: 7

190 assumed to cancel out in the annual mean, which is what we used in our analysis. With the
191 assumption that random errors cancel out, only systematic errors related to tropospheric
192 vertical column contents remain; these systematic errors do not contribute to uncertainty
193 in trend analyses. In addition, we first take monthly averages based on all daily
194 observations within a given month before calculating seasonal means to minimize any
195 potential effects of temporal variability in cloud cover.

196 -The Tropical Rainfall Measuring Mission (TRMM) daily precipitation product (3B42)
197 is based on a combination of TRMM observations, geo-synchronous infrared observations,
198 and rain gauge observations (Huffman et al., 2007). Independent rain gauge observations
199 from West Africa have been used to validate the product, with no indication of bias in the
200 product (Nicholson et al., 2003).

201 - NOAA Global Surface Temperature Dataset, a 0.5° gridded 2m monthly land surface
202 temperature product (Fan and van den Dool, 2008). The data set is based on a combination
203 of station observations from the Global Historical Climatology Network version 2 and the
204 Climate Anomaly Monitoring System (GHCN_CAMS), and uses an anomaly interpolation
205 approach which relies on observation-based reanalysis data to derive spatio-temporal
206 variation in temperature lapse rates for topographic temperature adjustment.

207 - 500m MCD64A1 collection 6 Moderate Resolution Imaging Spectroradiometer
208 (MODIS) burned area product for the period 2008-2018, (Giglio et al., 2018). The burned
209 area data are aggregated by month and gridded to 0.25° resolution, and do not include
210 burned area from small fires.

211 - MODIS MCD12C1 (collection 5) land cover product, which provides the percentage
212 of cropped area in each 0.25° grid cell (Friedl et al., 2002). In Africa, agriculture is often
213 practiced in complex mosaics of agricultural and natural land cover, so we used both the crop
214 and crop/natural area mosaic MODIS classifications as agricultural area in our analysis.

215 -We also used data on the spatio-temporal distribution of armed conflict events from
216 the Armed Conflict Location & Event Data Project (ACLED; Raleigh et al., 2010). We included
217 data for both violent and non-violent conflict events over the period 2008-2017.

Deleted: We used the

Deleted: We used the

Deleted: 7

Deleted: We also used the

2.2 Sudd wetland extent

Monthly flooded area extents of the Sudd Wetland, [South Sudan](#) from 2000 to 2017, were derived from 8-day composite MODIS land surface reflectance imagery (MOD09A1); data from 2005 through 2017 were used in the analyses. We refer to Di Vittorio and Georgakakos (2018) for a detailed description of the classification procedure designed to retrieve these data. In summary, monthly flood maps were obtained through a two-stage classification procedure. The first stage used the full 18-year data set to produce a wetland land cover map that distinguishes between wetland vegetation classes and their flooding regimes (permanently flooded, seasonally flooded, or non-flooded). The second stage compares seasonally flooded pixels from each vegetation class to their non-flooded counterparts on a monthly basis to identify the timing and duration of flooding for each pixel. These data were originally derived to calibrate a hydrologic model of the Sudd that is dependent on Nile flows; therefore, a connectivity algorithm was applied to ensure that all flooded pixels were physically connected to the Nile River. A few adjustments have been made to the previously published dataset for the application of this study. The classification algorithm has been improved to more accurately capture the inter-annual fluctuations in the permanently flooded areas. The dataset was also extended through 2017, and the total flooded area was quantified prior to applying the connectivity algorithm. The magnitudes of the monthly flooded area estimates are now substantially larger because they include areas flooded from local runoff in addition to areas flooded by the Nile River.

Deleted: 8

Deleted: the end of

2.3 Spatial and national analyses

We evaluated spatial relationships between mean annual tropospheric NH_3 concentration and several independent variables at 0.25° resolution: population density, livestock density, and cropped area. [Population density and livestock density data are not available as time series suitable for trend analysis, so we use single year values in our analyses.](#) We calculated population density based on the 2017 version of the US Department of Energy's Gridded Landscan population dataset (Dobson et al., 2000;

available at <https://landscan.ornl.gov>). Livestock density was based on the FAO global gridded livestock dataset for the year 2007 (Robinson et al., 2014). Before analysis, we converted the livestock densities of chickens, goats, pigs, and sheep to tropical livestock units (TLU), using values of 0.01, 0.1, 0.2, and 0.1 TLU, respectively; North African cattle were converted using a factor of 0.7, whereas sub-Saharan cattle were converted using a factor of 0.5 (Chilonda and Otte, 2006). For cropped area, we used the MODIS MCD12C1 (collection 5) land cover product as described above. We conducted spatial analyses by establishing a map of 1.5° grid cells and calculating the correlation between the value of each independent variable and NH₃ for all 0.25° grid cells within the larger grid cells (N = 144 including water grid cells, though these were excluded from the analysis).

National data on annual livestock numbers, crop production, and fertilizer N use were obtained from the UN Food and Agriculture Organization FAOSTAT for 51 African countries (FAO, 2020). Livestock data consisting of sheep, goats, cattle, and pigs were converted to tropical livestock units as described above, and buffaloes were converted using a conversion factors of 0.7 (Chilonda and Otte, 2006). [National emissions of CO₂ were obtained from World Bank Open Data](#) (World Bank, 2019). National-level mean annual cropland area, burned area, and atmospheric NH₃ and CO concentrations were also calculated for each of the 51 countries from the spatial datasets described above. Countries were sorted into three bins based on whether their relative change in mean annual NH₃ concentration was low, medium or high, and means and standard errors were calculated for each of the three 17-country bins.

Linear trend analyses were conducted using linregress from the scipy.stats package in Python v3.6.3. Statistical analyses of national scale data were conducted using ANOVA in R. Data were log [or rank](#) transformed when necessary to meet the assumptions of ANOVA. Values of α for treatment comparisons following significant ANOVA results were corrected for multiple testing using Benjamini-Hochberg corrections.

3. Results & Discussion

Field Code Changed

Deleted: n.d.

Deleted: , and in cases where assumptions were not met following transformations, the Kruskal-Wallis test was used...

3.1 Continental distributions and trends

Mean annual NH_3 concentrations for 2008-2018 are highest across the savannas and forest-savanna mosaics in North equatorial Africa, and especially in West Africa; there are smaller regional hotspots in the Lake Victoria basin, South Sudanese wetlands, and along the Nile delta and river (Fig. 1a). Parts of these regions experience substantial biomass burning (Fig. 1e), high livestock densities (Fig. 1g), and or high cropland cover (Fig. 1h), all of which can contribute to NH_3 emissions. The high concentrations in West Africa, which is one of the major global NH_3 hotspots (Van Damme et al., 2018), is likely the result of biomass burning emissions. Biomass burning emissions tend to drive seasonal variation in NH_3 VCDs in West Africa, with the largest emissions occurring late in the dry season and early rainy season (Hickman et al., *in review*). In addition to local emissions, biomass burning emissions and their reactive products are transported to the coast of West Africa during both the northern hemisphere rainy season, when it is transported from central and southern Africa, and during the dry season, when it is transported from biomass burning regions to the east (Sauvage et al., 2007). Most areas with trends are significant at $P=0.2$ or higher (Fig. S1).

In addition to being hotspots of mean NH_3 concentrations, some of these regions have also experienced increases in NH_3 concentrations from 2008 to 2018 (Fig. 1b). Like Warner et al. (2017) and Van Damme et al. (2021), we observed some increases in the northern grasslands, central African forests, and the Nile region, but we also observe trends in the Lake Victoria Basin, which Warner et al. (2017) did not, but Van Damme et al. (2021) did. Also in contrast to Warner et al. (2017) but in line with Van Damme et al. (2021), we observe a prominent decline in NH_3 VCDs over South Sudan (Fig. 1b, S1). We evaluate several of these regions in more detail below.

Deleted: 7

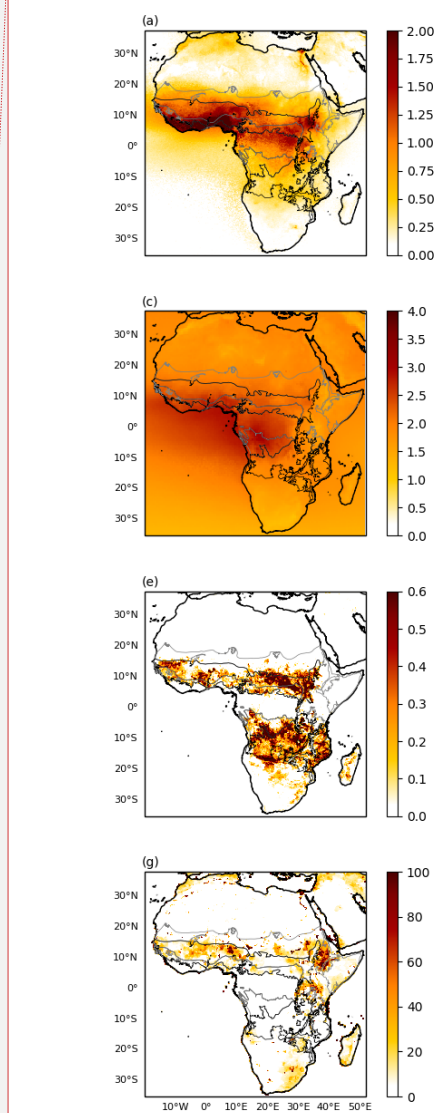
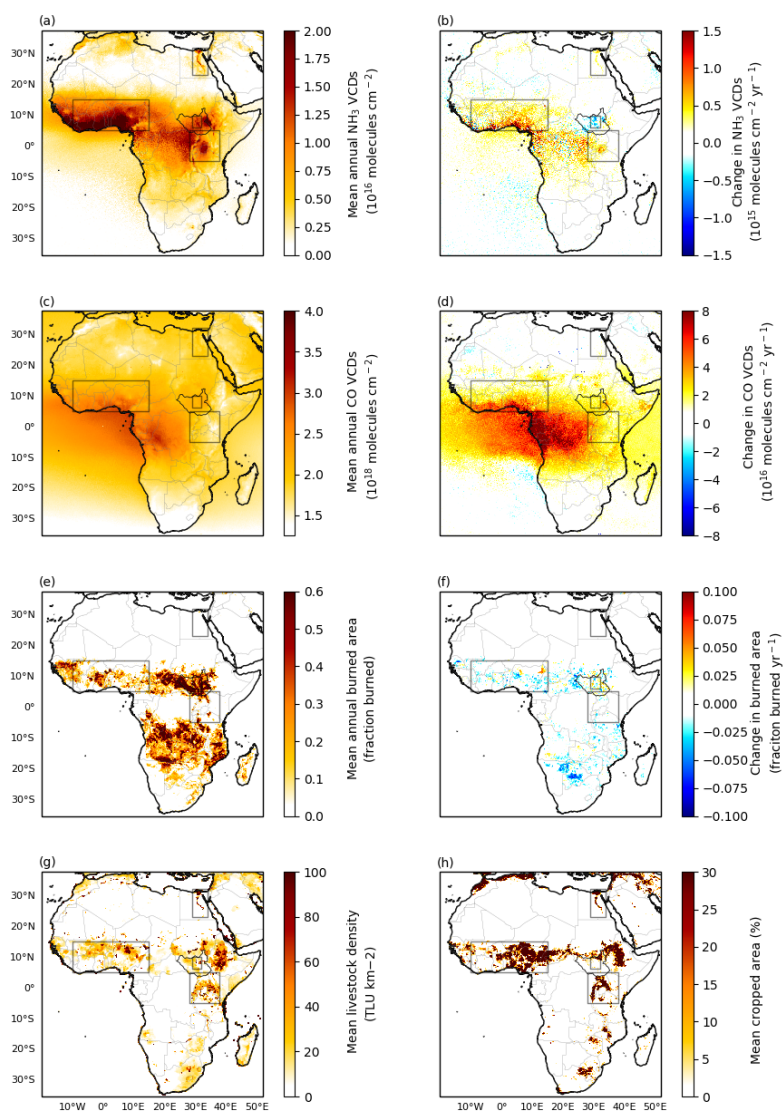
Deleted: S

Deleted: 7

Deleted: d

Deleted: and

Deleted: We also do not observe consistent changes over central African forests, where Warner et al. (2017) observed substantial increases in NH_3 VCDs.



Deleted:

Figure 1. Annual averages and trends in atmospheric NH_3 VCDs, CO VCDs, and burned area, as well as spatial distribution of livestock density and cropped area across seven sub-Saharan African ecoregions. Mean annual (a) and trend (b) in atmospheric NH_3 VCDs from IASI for the period 2008 through 2018. Mean annual (c) and trend (d) in annual atmospheric CO VCDs from IASI for the same period. Mean annual (e) and trend (f) in annual burned area from MODIS for 2008–2018. Livestock densities for 2007 from the FAO (f), and mean cropped area from MODIS for 2008–2018 (g). The border of South Sudan is highlighted in black, and several regions boxed: the Nile region at 30°N , the Sudd wetland in South Sudan, the Lake Victoria region at the equator, and West Africa centered around 10°N .

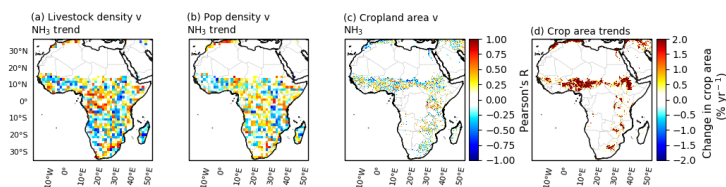
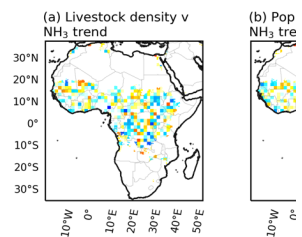


Figure 2. Relationships between NH_3 trends and livestock density, population density, and cropland area, as well as changes in cropland area. Spatial correlations between changes in annual atmospheric NH_3 VCDs and livestock density (a) and population density (b). Correlation between cropland area and NH_3 VCDs for 2008 through 2018 (c). Change in crop area for 2008 through 2018 (d). The NH_3 and crop area trends are based on data for 2008 through 2018, livestock density data are for the year 2007, population density data are for the year 2017.



Deleted: Livestock density and

Deleted: a

Deleted: burned area and

Deleted: concentrations

Deleted: 7

Deleted: 7

Deleted: key for the outlines of seven major African ecoregions...

Deleted:

Deleted: mean

Deleted: concentrations

Deleted: ,

Deleted: , and mean

Deleted: ,

Deleted: as well as trend

Deleted: 6

Deleted: In correlations,

Deleted: is

Deleted: 7

Deleted: , and cropland area are the mean of 2008 through 2016...

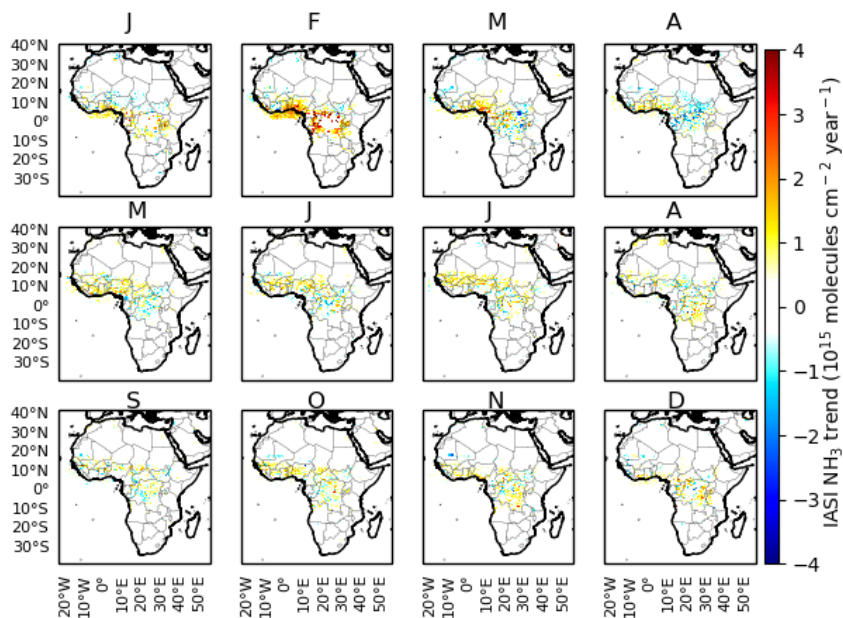
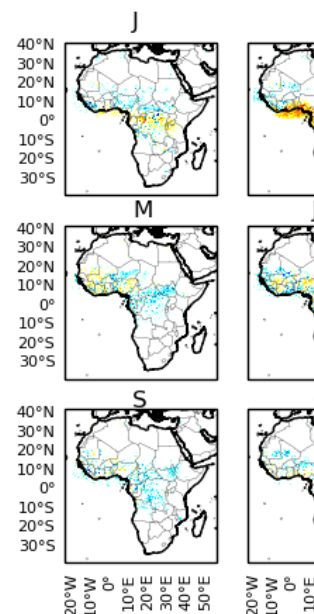
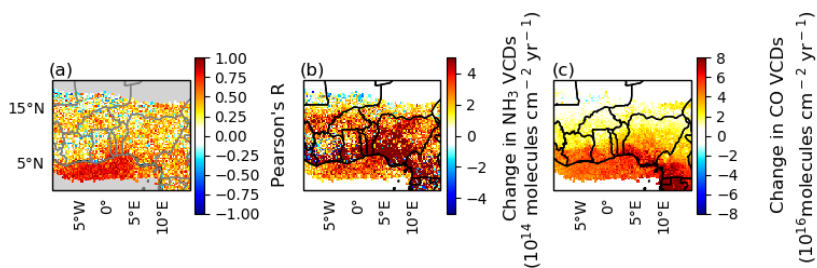
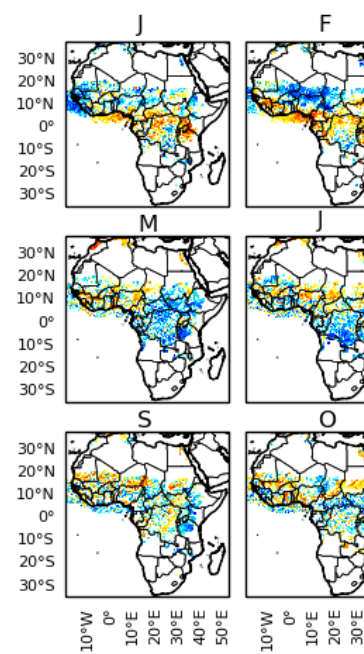


Figure 3. Change in mean monthly atmospheric NH_3 VCDs for the period 2008 through 2018. Grid cells where mean annual NH_3 VCDs for the entire period are under 5×10^{15} molecules cm^{-2} are not displayed. Results significant at $P=0.05$ are presented in Figure S2.



Deleted:

Deleted: 7



Deleted:

372

373 **Figure 4.** Correlation coefficient for the relationship between mean annual CO and
 374 NH₃ VCDs (a), changes in NH₃ VCDs (b) and changes in CO VCDs (c) over 2008 through
 375 2018 in West Africa. Grid cells where mean annual NH₃ VCDs for the entire period are
 376 under 5x10¹⁵ molecules cm⁻² are not displayed. Results significant at P=0.05 for the entire
 377 continent are presented in Figure S5.

378

379 3.2 West Africa

380 The increasing trend in NH₃ VCDs over West Africa are centered over Nigeria and
 381 the southern coast, and to a lesser extent across parts of the wet savanna (Fig. 1b).
 382 Increases in NH₃ VCDs tend to be higher in grid cells with higher population densities in
 383 Nigeria (Fig. 2b), suggesting a possible anthropogenic influence. The spatial distribution of
 384 the mean annual NH₃ trend is overlapped by a substantial increase in mean annual CO
 385 VCDs (Fig. 1b, 1d), pointing to a biomass burning source, as is also the case in central Africa.
 386 Earlier studies have found substantial declines in annual burned area across the north
 387 equatorial African biomass burning region as detected by MODIS (Andela et al., 2017;
 388 Andela and Van Der Werf, 2014) and related declines in NO₂ VCDs across the region
 389 (Hickman et al., in review; Hickman et al., 2021), which would seem to stand in contrast to
 390 the increasing CO and NH₃ trends observed here.

391 However, the annual decline in burned area and NO₂ VCDs is characterized by
 392 heterogeneity when considering individual months. In West Africa, the dry season is
 393 typically November to February or March. During the transition from the dry to rainy
 394 season in February and March, NO₂ VCDs exhibit increasing rather than decreasing trends
 395 in West Africa, though burned area patterns are not as clear when 2018 is included
 396 (Hickman et al., 2021; Fig. S2, S3). Although these increases in NO₂ VCDs are small in the
 397 annual context, they occur at a time of year when biomass burning combustion is less
 398 complete, potentially due to greater fuel moisture and declining fire radiative power
 399 (Hickman et al., 2021; Zheng et al., 2018). These conditions would lead to greater

Deleted: 7

Deleted: Regions

Deleted: screened out

Field Code Changed

Deleted: :

Deleted: d

Deleted: between

Deleted: and

Deleted: s

Deleted: both

Deleted: and burned area

Field Code Changed

Deleted: , leading to greater emissions of less oxidized species such as CO and NH₃, rather than the more fully oxidized species such as CO₂ and NO₂ that dominate emissions during the peak of the biomass burning season

414 ~~emissions of less oxidized species such as CO and NH₃, rather than the more fully oxidized~~
415 ~~species such as CO₂ and NO₂ that dominate emissions during the peak of the biomass~~
416 ~~burning season (Fig. S2, S4).~~ Indeed, our observations suggest that much of the increasing
417 NH₃ trend occurs during this transitional period, with NH₃ VCDs increasing by roughly 7%
418 yr⁻¹ for all of Nigeria during February and March (Fig. 3; ~~p<0.01~~). Variation in NH₃ VCDs
419 are positively correlated with CO VCDs (Fig. 4a, S5), which are also increasing during this
420 period (Fig. 4c, S4).

Deleted: 6

421 These correlations imply a biomass burning source for the increasing NH₃ VCDs in
422 West Africa; ~~although the burned area trends are not as clear, it is important to remember~~
423 ~~that MODIS undercounts burned area during this time of year by a factor of 3 to 6, and so~~
424 ~~would be less sensitive to trends~~ (Ramo et al., 2021; Roteta et al., 2019). ~~Although there is~~
425 ~~considerable gas flaring in Nigeria, gas flaring emissions have exhibited long-term negative~~
426 ~~trends~~ (Doubmbia et al., 2019). ~~In addition, although NO₂ VCDs were found to decrease~~
427 ~~across the productive savannas of West Africa, regions of increasing NO₂ VCDs were~~
428 ~~observed over large parts of Nigeria, further suggesting that there may be increases—or at~~
429 ~~least smaller decreases—in biomass burning in the country~~ (Hickman et al., 2021). It is
430 unlikely that changes in chemical sinks—specifically, the formation of nitrate aerosols in
431 reactions with NO_x or sulfate—are responsible for the ~~increasing~~ trend: the observed
432 increase in NO₂ VCDs observed during February and March would be expected to lead to a
433 shorter NH₃ lifetime and ~~decreasing~~ VCDs. In addition, emissions of SO₂ are relatively low
434 in West Africa, with moderate emissions occurring in Nigeria, but neither emissions nor
435 lifetime exhibit clear seasonal variation (Lee et al., 2011).

Deleted: 2

436 Small agricultural fires are likely an important contributor to the increasing NH₃
437 VCDs during the dry-to-rainy season transitional period—a period when agricultural fires
438 are common in the region (Korontzi et al., 2006). There are large numbers of small fires
439 that are not detected by MODIS during these months: ~~as noted above~~, estimates of burned
440 area during February, March, and April are revised upwards by roughly a factor of 3 to 6
441 over MODIS when small fires are included (Ramo et al., 2021; Roteta et al., 2019). Many of
442 these small fires are likely related to agricultural field preparation prior to planting
443 (Gbadegesin and Olusesi, 1994), which typically takes place in March or April (Vrieling et
444 al., 2011; Yegbemey et al., 2014). An increase in fires during this transitional period is also

Deleted: lower

consistent with one of the primary mechanisms behind the overall decline in burned area: roughly half of the decline is attributed to increased population density and the expansion of agricultural area, which contributes to the anthropogenic suppression of larger fires (Andela et al., 2017; Andela and Van Der Werf, 2014). This agricultural expansion, however, can be expected to be accompanied by increases in small fires used for the removal of stubble or harvest byproduct (Gbadegesin and Olusesi, 1994), leading to the increased emissions during the rainy-to-dry season transition observed here.

Globally, agricultural emissions from fertilized soils and livestock excreta are the largest source of NH_3 (Bauer et al., 2016), and Warner et al. (Warner et al., 2017) suggest that national-scale changes in fertilizer use could explain the NH_3 trend over Nigeria. However, as noted above, much of the increase in West Africa occurs prior to the start of the planting season—before fertilizer is applied—and appears likely to be due to biomass burning emissions instead. Fertilizer or manure may make a contribution to the increasing trend later in the year, as NH_3 VCDs increase in the wet savanna during May, June, and July (Fig. 3), though there are also significant correlations between NH_3 and CO VCDs (Fig. 4), suggesting that biomass burning may continue to play an important role. However, average N fertilizer use in West Africa is universally under $40 \text{ kg N ha}^{-1} \text{ yr}^{-1}$, typically under $20 \text{ kg N ha}^{-1} \text{ yr}^{-1}$, and is under $10 \text{ kg N ha}^{-1} \text{ yr}^{-1}$ in Nigeria—over an order of magnitude lower than rates in Europe, the United States, and China (FAO, 2020). Although percentage changes in fertilizer use are substantial, in absolute terms they represent increases of less than $2 \text{ kg N ha}^{-1} \text{ yr}^{-1}$, and frequently less than $1 \text{ kg N ha}^{-1} \text{ yr}^{-1}$, a relatively small but perhaps not entirely trivial perturbation to the N cycle. Between 2000 and 2007, total N deposition averaged $8.38 \text{ kg N ha}^{-1} \text{ yr}^{-1}$ in wet savanna and $14.75 \text{ kg N ha}^{-1} \text{ yr}^{-1}$ in forest ecosystems based on surface sampling sites (Galy-Lacaux and Delon, 2014), and biological N fixation in tropical and wet savannas has been estimated as ranging from 16 to $44 \text{ kg N ha}^{-1} \text{ yr}^{-1}$ (Bustamante et al., 2006), suggesting that fertilizer increases may represent a 1 to 2% annual increase in N inputs. But given the small magnitude of fertilizer applications, it appears unlikely that changes in fertilizer use can explain the entirety of NH_3 increases during the growing season.

3.3. South Sudan

The most notable declining trend in NH_3 VCDs occurs in South Sudan over the Sudd wetlands at a rate of over $2\% \text{ yr}^{-1}$ (Fig. 1b; $p=0.20$). It appears that this decline is related to interannual variation in the flooded extent of the Sudd, a vast wetland that connects the White and Blue Nile tributaries. Seasonal variation of inflow to the Sudd leads to variation in flooded extent: an area of roughly $15,000 \text{ km}^2$ is permanently flooded, and another roughly $15,000 \text{ km}^2$ is temporarily flooded each year, with considerable interannual variation in the total flooded area (Di Vittorio and Georgakakos, 2018). Among other factors, drying soils should increase production and emissions of NH_3 from soils, as Eq. 1 is shifted to the right (Clarisse et al., 2019). Earlier work evaluating an NH_3 hotspot over Lake Natron in Tanzania found that the drying of seasonally flooded soils leads to large emissions of NH_3 : As the waters of Lake Natron recede during the dry season each year and the surrounding mud flats dry out, NH_3 VCDs increase rapidly, with hotspots appearing over the mudflats (Clarisse et al., 2019). These elevated VCDs are attributed to multiple possible factors, including the effects of drying on concentrations of NH_3 in solution (which increases the concentration gradient with the atmosphere), reduced biological uptake of NH_3 , convective transport of dissolved NH_3 from depth to the soil surface, and increased mineralization of labile organic matter (Clarisse et al., 2019).

We find the same clear seasonal relationship between wetland flooded extent and NH_3 concentrations over the Sudd—VCDs increase as waters recede from the temporarily flooded area, leading to annual maxima from February through May (Fig. 5a; bounding box of 29E to 31.5E and 6N to 9.9N). Like the entire country, seasonal variation in NH_3 VCDs over the Sudd follow variation in surface temperature, but NH_3 concentrations over the Sudd are substantially elevated compared to surrounding regions during this time of year but not others, suggesting that an mechanism in addition to temperature is contributing to the elevated emissions in the Sudd during February through May, a period that spans the end of the dry season and start of the rainy season (Fig. S6). This conclusion is supported by an analysis of interannual variation of VCDs during the February through May period. Interannual variation in NH_3 VCDs is largely decoupled from variation in temperature, but

Deleted: ,

Deleted: during the February through May period

Deleted: additional

Deleted: 3

Deleted: .

NH₃ VCDs appear to vary inversely with the amount of area that dries out each year (Fig. 5b). Over the period for which flooded extent data are currently available for the Sudd, the minimum flooded extent tends to increase—that is, less area dries out each year—resulting in an overall decline in NH₃ VCDs. Linear regression reveals that this change in flooded extent explains a large proportion of the annual variation in NH₃ in the Sudd bounding box ($r=-0.65$, $p=0.04$) as well as for the country as a whole ($r=-0.63$, $p=0.05$). These analyses strongly suggest that the declining trend in NH₃ over the Sudd is a direct result of an overall increase in the minimum flooded extent over the observation period.

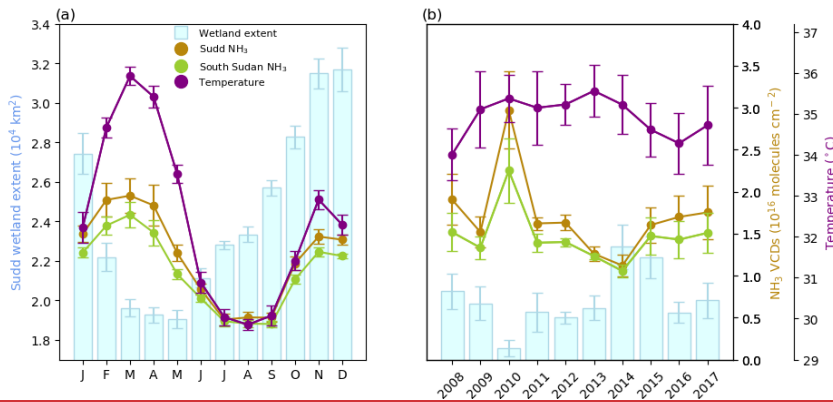
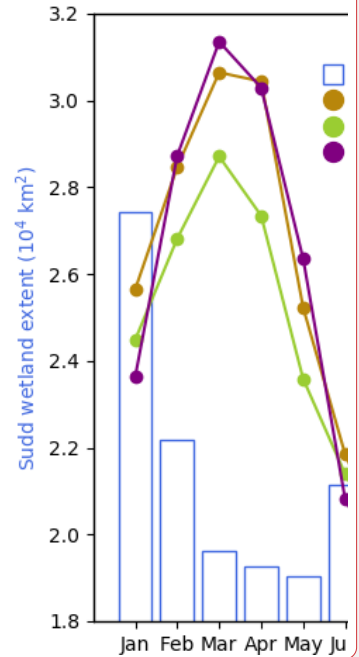


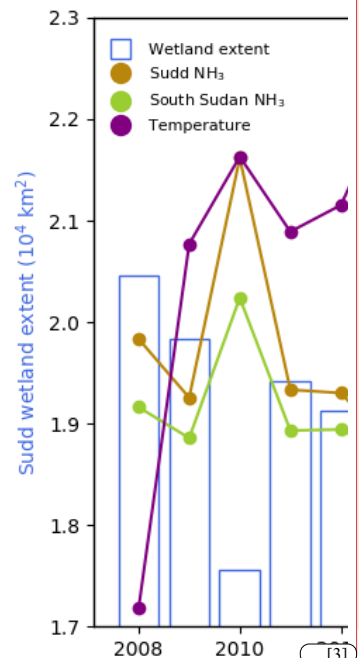
Figure 5. Mean (a) monthly and (b) February through May annual mean flooded extent of the Sudd, surface temperatures over South Sudan, and NH₃ VCDs over the Sudd and the entirety of South Sudan for the period 2008 through 2017.

Deleted: 6.... Over the period for which flooded extent data are currently available for the Sudd, the minimum flooded extent tends to increase—that is, less area dries out each year—resulting in an overall decline in NH₃ VCDs. Linear regression reveals that this change in flooded extent explains a large proportion of the annual variation in NH₃ in the Sudd bounding box ($r=-0.659$, $p=0.03$)

Deleted: 70... $p=0.02$)... ..during February through



Deleted:



Deleted:

Formatted: Indent: First line: 0"

565 It is possible that conflict in South Sudan could contribute to the decline in NH₃
566 VCDs. In 2013, a civil conflict emerged in South Sudan that was ultimately responsible for
567 the displacement of millions of people (Global Internal Displacement Monitoring Centre,
568 2020; World Bank, 2019) and the disruption of livestock migration patterns (Idris, 2018).
569 However, these disruptions appeared only after the onset of the long-term change in NH₃,
570 and appear unlikely to make an important contribution to the observed interannual
571 variation (SI Text, Fig. S7, S8).

572 It is unlikely that changes in chemical sinks are responsible for the decline in NH₃
573 VCDs. VCDs of tropospheric NO₂ are also decreasing in the region (Fig. S9), which is
574 suggestive of less formation of particulate-phase ammonium rather than more.
575 Anthropogenic SO₂ emissions in Africa in general and South Sudan in particular are very
576 low (European Commission Joint Research Centre (JRC)/Netherlands Environmental
577 Assessment Agency (PBL), 2016), and would not be expected to be emitted from the Sudd;
578 more generally, the clear spatial association between the NH₃ trend and the Sudd (Fig. 1,
579 Fig. S10) is strongly suggestive of changes in emissions rather than atmospheric processes
580 being responsible for the trend.

582 3.4 Lake Victoria Basin region

583 The Lake Victoria Basin and its surroundings—an area including elevated mean NH₃
584 VCDs—exhibit an increasing NH₃ trend (Fig. 1b, Fig. 7, Fig. S11), which appears to be the
585 result of increasing agricultural activity in the area. The region includes a high and
586 increasing density of agricultural land (Fig. 1h, Fig. 2d, Fig. S12), and these increases in
587 cropped area are positively correlated with increases in NH₃ VCDs across much of the
588 region (Fig. 2c). The northern and southern halves of the Lake Victoria region have distinct
589 growing seasons: in the north, the season generally starts in April, whereas in the south, it
590 starts in November or December (Vrieling et al., 2011). The long-term trend reflects this
591 seasonality, with increases in the north and south occurring during their respective
592 growing seasons (Fig. 3). Fertilizer use in the Lake Victoria region is low: national averages

Deleted: These disruptions could be expected to lead to a decrease in NH₃ VCDs if they result in lower rates of fertilizer use and a decrease in livestock and livestock-related emissions. Although there are some spatial correspondences between the location of conflict events and changes in NH₃ VCDs (Fig. S4), the change in NH₃ VCDs appears already to have been underway years in advance of the onset of conflict (Fig. 6, Fig. S5), suggesting that other factors are responsible for the interannual variation. Displacement spiked in 2014, the year that NH₃ VCDs were at their lowest values. It is possible that this displacement and the associated conflict contributed to the low NH₃ values, but 2014 was the year of the largest Sudd extent during February through May, which would also be expected to reduce NH₃ emissions. The number of refugees and internally displaced people increased substantially from 2013 through 2017, a period during which the dry season flooded extent of the Sudd decreased, and NH₃ VCDs increased (Fig. S5). Maps of annual mean NH₃ VCDs over the IASI lifetime reveal that a large amount of the interannual variability occurs over the Sudd (Fig. S6), though there is also variability in other parts of the country, though these do not map strongly to interannual variability in precipitation (Fig. S7). The strong spatial relationship between the Sudd and interannual NH₃ variability suggests that Sudd flooded extent is likely the main factor responsible for the interannual variation in NH₃ VCDs during this period, and the overall trend we observe for 2008 through 2017.

Deleted: 8

Deleted: 6

Deleted: 9

Deleted: Fig. S1,

Deleted: 0

range from about 1 to 3 kg nutrients ha⁻¹ yr⁻¹ in Uganda to about 35 to 40 kg nutrients ha⁻¹ yr⁻¹ in Kenya (Elrys et al., 2019; World Bank, 2019); to put these numbers in context, Organization for Economic Cooperation and Development (OECD) countries use about 135-140 kg nutrients ha⁻¹ yr⁻¹ (World Bank, 2019). Although rates of fertilizer use have increased by substantial proportions, the absolute amount of increase is relatively small, typically roughly 1 to 10 kg nutrients decade⁻¹. Unlike in West Africa, however, interannual variation in burned area (Fig. S13) does not exhibit a clear relationship with changes in NH₃ VCDs. Consequently, we expect that both the expansion and intensification of agriculture in the region contribute to the increasing NH₃ VCDs.

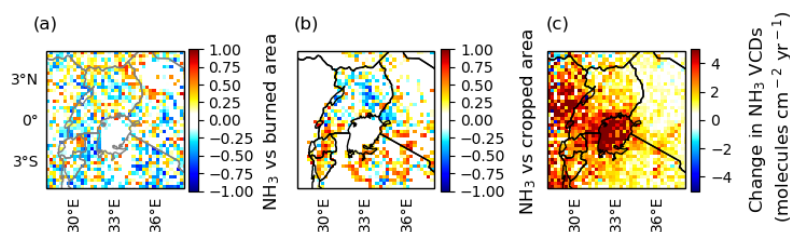
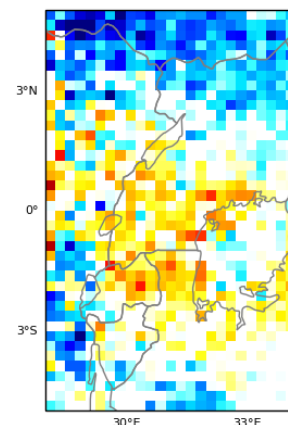


Figure 7. Changes in NH₃ VCDs and their relationship with burned area and cropped area over the Lake Victoria region for the 2008 through 2018 period. (a) Correlation coefficients for the relationship between NH₃ VCDs and burned area. (b) Correlation coefficients for the relationship between NH₃ VCDs and cropped area, including mosaics of crops and natural vegetation cover. (c) Changes in NH₃ VCDs.

3.5 National-scale relationships

Examining relationships at a national scale can provide insight into relationships between changes in agricultural or biomass burning and changes in atmospheric NH₃ VCDs at larger scales. When grouping countries into three bins based on their annual percentage changes in NH₃ VCDs, there is some evidence for a broad relationship between livestock and NH₃ VCDs at the national scale (Fig. 8). The rate of change in national-scale NH₃ VCDs varies significantly among bins ($p < 0.001$; rank transformed). The annual percentage



Deleted:

Deleted: Change in mean annual NH₃ VCDs

Deleted: ,

Deleted: 7

Deleted: agriculture

Deleted: becomes apparent

Deleted: , though in no bins is the rate of change positive

changes in livestock in TLUs vary significantly by bin ($p=0.056$), with the middle bin higher than the bottom bin ($p=0.03$) and the high bin higher than the bottom bin, though not significantly so ($p=0.21$). Annual percentage changes in fertilizer N ($p=0.23$) and crop production ($p=0.62$; rank transformed) did not vary by bin.

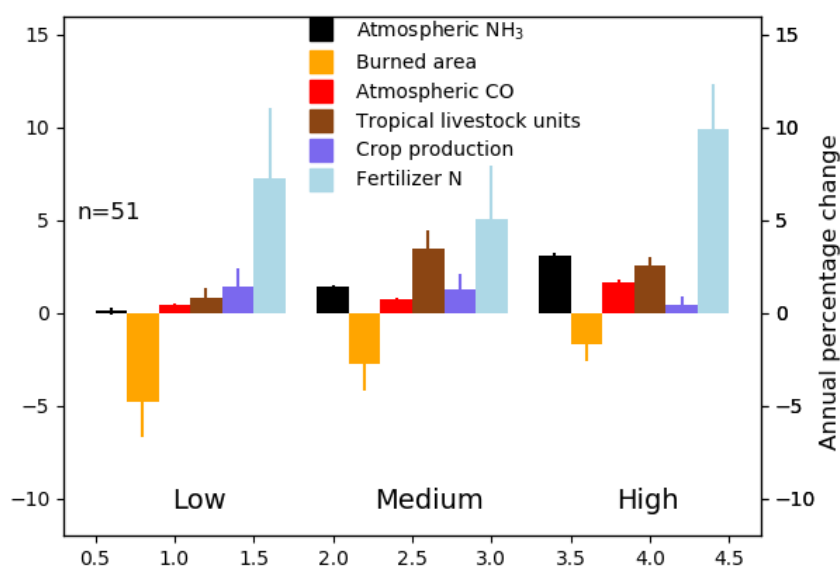


Figure 8. Annual percentage changes in national mean annual NH₃ VCDs, burned area, CO VCDs, livestock, crop yield, and fertilizer N use for African countries with low, medium, or high rates of NH₃ VCD change. Error bars represent the standard error of the mean. See Table S1 for the list of countries in each bin and Fig. S14 for an expanded set of variables.

Instead of a direct agricultural relationship with changes in NH₃ VCDs, there is the possibility that changes in biomass burning are associated with changes in NH₃ VCDs. Although the differences in the annual percentage change in burned area were not

Deleted: of national gross production ($p=0.009$) and

Deleted: ($p=0.003$)

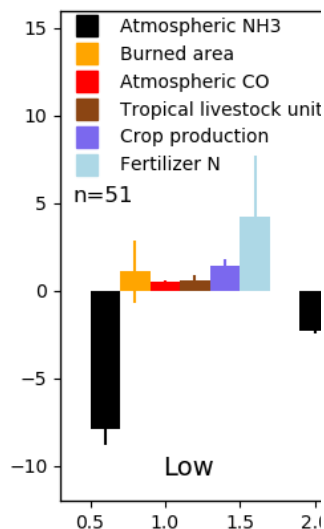
Deleted: whereas

Deleted: a

Deleted: use are not quite significantly different across bins

Deleted: 18

Deleted: Nevertheless the general pattern suggests that countries with greater agricultural activity tend to have smaller declines in NH₃ VCDs.



Deleted:

Deleted: addition to these

Deleted: s

Deleted: also

Deleted: a

significant among bins ($p=0.48$; rank transformed), the overall pattern is consistent with earlier results finding that a reduction in burned area across the northern biomass burning region was associated in part with the expansion of agriculture and presumed anthropogenic suppression of fire (Andela et al., 2017; Andela and Van Der Werf, 2014). However, burned area as measured by MODIS is likely an imperfect predictor for NH_3 emissions—as noted previously, MODIS underestimates burned area by a factor of 3 to 6 during shoulder seasons (Roteta et al., 2019), which is when fires are expected to emit more reduced species such as NH_3 (Zheng et al., 2018). In contrast to burned area, the annual change in column densities of CO—which tends to be co-emitted with NH_3 from fires—differed significantly among bins ($p<0.001$; rank transformed) and was significantly higher in the high bin than in the low or medium bins. ($p<0.001$, post-hoc tests). The higher annual CO changes in the high bin could related to larger anthropogenic fossil fuel emissions, but we see no difference among bins in growth rates of CO_2 emissions ($p=0.45$; Figure S14); such a difference would be expected if differences in economic development were responsible for the CO differences. These results leave open the possibility that changes in either biofuel emissions or biomass burning emissions—perhaps from smaller fires not observed in the MODIS burned area product—may be primarily responsible for the difference in CO between bins, and may be contributing to the differences in NH_3 between bins. Changes in NO_2 VCDs and SO_2 concentrations can affect the lifetime of NH_3 (the latter by changing SO_4 concentrations), but do not appear to make an important contribution to the observed trends in NH_3 VCDs among bins (Fig. S14, SI text). Temperature, likewise, does not appear to play an important role (SI text).

4. Conclusion

Using IASI, we have observed both increases and decreases in atmospheric NH_3 VCDs in different regions in Africa between 2008 and 2018, with different factors affecting trends in different regions.

We observed increases in NH_3 VCDs in West Africa, which earlier work had concluded was likely related to increased fertilizer use. Fertilizer is not typically applied in West Africa until the start of the growing season—often April—but we find that much of the NH_3 increase occurs during February and March, suggesting that increasing fertilizer

Deleted: 61

Deleted: Indeed, many of the countries in the high bin—where burned area exhibits a declining trend—are from that biomass burning region (Table S1).

Deleted: of

Deleted: 0

Deleted: per capita GDP

Deleted: 24

Deleted: 7

Deleted: most

730 use is unlikely to provide a complete explanation for the NH₃ trend. Agriculture may
731 nevertheless play a role, with enhanced burned area and especially CO concentrations in
732 February suggestive of increased burning of crop stubble in preparation for planting during
733 this time of year. Fires in this region tend to emit a greater proportion of less oxidized
734 species such as NH₃ at the end of the dry season, consistent with a biomass burning source
735 for the increasing NH₃ VCDs.

736 Decreases in NH₃ VCDs were largest in South Sudan, especially over the Sudd
737 wetland, where NH₃ VCDs vary seasonally with the extent of area flooded. As the
738 temporarily flooded areas of the Sudd dry out each year, NH₃ VCDs increase as reduction in
739 soil moisture drives increased production and volatilization of NH₃. The area of the Sudd
740 that is flooded each year varies, and from 2008 ~~until 2015~~, the area that remains flooded
741 during the dry season generally increased, ~~producing a positive overall trend for the period~~
742 ~~of 2008 through 2017~~. This increase in the dry season flooded area drove a decrease in
743 NH₃ VCDs: with less soil drying out, the seasonal maxima in NH₃ VCDs were lower.
744 Although it is possible that conflict in South Sudan could contribute to changes in NH₃
745 VCDs, the timing and distribution of conflict events and human displacement suggest that
746 other factors are likely more important.

747 Modest increases in NH₃ VCDs were observed in the Lake Victoria region. This
748 region has experienced increases in agricultural area during the IASI observation period,
749 and these changes explained a large proportion of the variation in NH₃ VCDs across large
750 patches of the region, where biomass burning could not. We expect that both expansion
751 and intensification of agriculture in this region could contribute to the positive NH₃ trend.

752 Considering national-scale statistics, ~~comparisons~~ between equally sized bins of 17
753 countries each ~~suggested that changes in biomass burning emissions and livestock~~
754 ~~emissions could contribute to differences in NH₃ VCDs among countries, but variables~~
755 ~~related to cropped agriculture such as cropped area or fertilizer N use did not appear to be~~
756 ~~important factors at this scale. This may be because~~ although fertilizer use has been
757 increasing in sub-Saharan Africa, it remains extremely low relative to other continents, and
758 relative to the levels needed to attain food security. Average fertilizer use in most
759 countries in the region is under 20 kg N ha⁻¹ ~~yr⁻¹~~, and sometimes less than 5 kg N ha⁻¹ ~~yr⁻¹~~.
760 Although recommended fertilizer rates are lower in most African countries than in the U.S.

Deleted: through

Deleted: 4

Deleted: most countries showed an overall decline in mean annual NH₃ VCDs over the observation period. Comparisons

Formatted: Indent: First line: 0"

Deleted: revealed an inverse relationship between NH₃ VCDs and rates of change in agricultural variables such as livestock, crop production, and

Deleted: (though not quite significant) N fertilizer use—generally, greater rates of increase in agricultural variables were associated with smaller decreases in NH₃ VCDs. ¶ However, even

or Europe, increasing N inputs to 50, 100, or 150 kg N ha⁻¹ ~~yr⁻¹ would~~ represent a major perturbation to the regional N cycle, and potentially a large new source of NH₃ to the atmosphere. West Africa is already a global NH₃ hotspot (Van Damme et al., 2018), suggesting that encouraging policies that can help to limit NH₃ emissions during the early stages of agricultural intensification in Africa may help mitigate potential impacts on the atmosphere. Fortunately, agricultural practices such as sub-surface application of fertilizer, which is already being promoted to smallholder farmers, can serve to both limit NH₃ emissions also help to increase crop yields.

These past and anticipated future trends also make the case for expanding capacity for atmospheric monitoring in sub-Saharan Africa. Although long-term monitoring networks have been established in West Africa (Adon et al., 2010; Ossouhou et al., 2019) and South Africa (Conradie et al., 2016) ~~as part of the INDAAF network, it is mainly focused on deposition.~~ the spatio-temporal resolution of surface measurements is very coarse when compared to the data available in other parts of the world, and will limit our ability to understand how agricultural and socio-economic development in Africa affect the atmosphere. Satellite observations can help to bridge some of these data gaps, but have their own spatio-temporal limitations, and would further benefit from additional high-quality surface observations for evaluation of retrieval products.

Data availability: All data used in this study are available from public sources, with the exception of Sudd wetland extent, which is available by request from Courtney Di Vittorio. The IASI NH₃ and CO data are available from The IASI <https://iasi.aeris-data.fr>. The NOAA Global Surface Temperature Dataset is available at <https://data.nodc.noaa.gov/cgi-bin/iso?id=gov.noaa.ncdc:C01585>. MODIS burned area data are available from <https://www.globalfiredata.org/data.html>. MODIS agricultural area are available at <https://lpdaac.usgs.gov/products/mcd12c1v006/>. TRMM 3B42 precipitation data are available from <https://pmm.nasa.gov/data-access/downloads/trmm>. The Gridded Livestock of the World data are available from <https://livestock.geo-wiki.org/home-2/>. Population density data for 2017 are available at <https://landscan.ornl.gov/downloads/2017>. FAO national crop production and fertilizer N data are available at <http://www.fao.org/faostat/en/>. Data on conflict events from

Deleted: s

805 ACLED are available at <https://acleddata.com/#/dashboard>. World Bank national statistics
806 on refugees and internally displaced people are available at <https://data.worldbank.org>.

807

808 **Author Contribution:** J.E.H. designed the study, conducted the analysis, and wrote the paper.
809 NA, ED, CD, MO, CG-L, KT, and SEB contributed to study design and edited the paper. LC, P-
810 FC, and MVD developed the original IASI trace gas retrievals and edited the paper.

811 The authors declare that they have no conflict of interest.

812

813 References

814 van der A, R. J., Eskes, H. J., Boersma, K. F., van Noije, T. P. C., Van Roozendael, M., De Smedt,
815 I., Peters, D. H. M. U. and Meijer, E. W.: Trends, seasonal variability and dominant NOx
816 source derived from a ten year record of NO2 measured from space, *J. Geophys. Res.*
817 *Atmos.*, 113(4), D04302, doi:10.1029/2007JD009021, 2008.

818 Adon, M., Galy-Lacaux, C., Yoboué, V., Delon, C., Lacaux, J. P., Castera, P., Gardrat, E., Pienaar,
819 J., Al Ourabi, H., Laouali, D., Diop, B., Sigha-Nkamdjou, L., Akpo, a., Tathy, J. P., Lavenu, F. and
820 Mougin, E.: Long term measurements of sulfur dioxide, nitrogen dioxide, ammonia, nitric
821 acid and ozone in Africa using passive samplers, *Atmos. Chem. Phys.*, 10(15), 7467–7487,
822 doi:10.5194/acp-10-7467-2010, 2010.

823 AGRA: AGRA in 2008: Building on the New Momentum in African Agriculture., 2009.

824 Andela, N. and Van Der Werf, G. R.: Recent trends in African fires driven by cropland
825 expansion and El Niño to la Niña transition, *Nat. Clim. Chang.*, 4(9), 791–795,
826 doi:10.1038/nclimate2313, 2014.

827 Andela, N., Morton, D. C., Giglio, L., Chen, Y., Van Der Werf, G. R., Kasibhatla, P. S., DeFries, R.
828 S., Collatz, G. J., Hantson, S., Kloster, S., Bachelet, D., Forrester, M., Lasslop, G., Li, F., Mangeon,
829 S., Melton, J. R., Yue, C. and Randerson, J. T.: A human-driven decline in global burned area,
830 *Science* (80-.), 356(6345), 1356–1362, doi:10.1126/science.aal4108, 2017.

831 Anker, H. T., Baaner, L., Backes, C., Keessen, A. and Möckel, S.: Comparison of ammonia
832 regulation in Germany , the Netherlands and Denmark – legal framework, Copenhagen.,
833 2018.

834 Bauer, S. E., Tsigaridis, K. and Miller, R.: Significant atmospheric aerosol pollution caused by
835 world food cultivation, *Geophys. Res. Lett.*, 43(10), 5394–5400,
836 doi:10.1002/2016GL068354, 2016.

837 Behera, S. N., Sharma, M., Aneja, V. P. and Balasubramanian, R.: Ammonia in the
838 atmosphere: A review on emission sources, atmospheric chemistry and deposition on
839 terrestrial bodies, *Environ. Sci. Pollut. Res.*, 20(11), 8092–8131, doi:10.1007/s11356-013-
840 2051-9, 2013.

841 Bouwman, A. F., Lee, D. S., Asman, W. A. H., Dentener, F. J., Van Der Hoek, K. W. and Olivier, J.
842 G. J.: A global high-resolution emission inventory for ammonia, *Global Biogeochem. Cycles*,
843 11(4), 561–587, 1997.

844 Bustamante, M. M. C., Medina, E., Asner, G. P., Nardoto, G. B. and Garcia-Montiel, D. C.:
845 Nitrogen cycling in tropical and temperate savannas, *Biogeochemistry*, 79(1–2), 209–237,
846 doi:10.1007/s10533-006-9006-x, 2006.

847 Cahoon, D. R., Stocks, B. J., Levine, J. S., Cofer, W. R. and O'Neill, K. P.: Seasonal distribution of
848 African savanna fires, *Nature*, 359(6398), 812–815, doi:10.1038/359812a0, 1992.

849 Chen, L.-W. A., Verburg, P., Shackelford, A., Zhu, D., Susfalk, R., Chow, J. C. and Watson, J. G.:
850 Moisture effects on carbon and nitrogen emission from burning of wildland biomass,
851 *Atmos. Chem. Phys.*, 10(14), 6617–6625, doi:10.5194/acp-10-6617-2010, 2010.

852 Chilonda, P. and Otte, J.: Indicators to monitor trends in livestock production at national,
853 regional and international levels, *Livest. Res. Rural Dev.*, 18(8), 1–12, 2006.

854 Clarisse, L., Clerbaux, C., Dentener, F., Hurtmans, D. and Coheur, P. F.: Global ammonia
855 distribution derived from infrared satellite observations, *Nat. Geosci.*, 2(7), 479–483,
856 doi:10.1038/ngeo551, 2009.

857 Clarisse, L., Van Damme, M., Gardner, W., Coheur, P.-F., Clerbaux, C., Whitburn, S., Hadji-
858 Lazaro, J. and Hurtmans, D.: Atmospheric ammonia (NH₃) emanations from Lake Natron's
859 saline mudflats, *Sci. Rep.*, 9, 4441, doi:10.1038/s41598-019-39935-3, 2019.

860 Conradie, E. H., Van Zyl, P. G., Pienaar, J. J., Beukes, J. P., Galy-Lacaux, C., Venter, A. D. and
861 Mkhathshwa, G. V.: The chemical composition and fluxes of atmospheric wet deposition at
862 four sites in South Africa, *Atmos. Environ.*, 146, 113–131,
863 doi:10.1016/j.atmosenv.2016.07.033, 2016.

864 Van Damme, M., Wichink Kruit, R. J., Schaap, M., Clarisse, L., Clerbaux, C., Coheur, P. F.,

865 Dammers, E., Dolman, A. J. and Erisman, J. W.: Evaluating 4 years of atmospheric ammonia
 866 (NH₃) over Europe using IASI satellite observations and LOTOS-EUROS model results, J.
 867 Geophys. Res., 119(15), 9549–9566, doi:10.1002/2014JD021911, 2014a.
 868 Van Damme, M., Clarisse, L., Heald, C. L., Hurtmans, D., Ngadi, Y., Clerbaux, C., Dolman, A. J.,
 869 Erisman, J. W. and Coheur, P. F.: Global distributions, time series and error characterization
 870 of atmospheric ammonia NH₃ from IASI satellite observations, Atmos. Chem. Phys., 14(6),
 871 2905–2922, doi:10.5194/acp-14-2905-2014, 2014b.
 872 Van Damme, M., Clarisse, L., Dammers, E., Liu, X., Nowak, J. B., Clerbaux, C., Flechard, C. R.,
 873 Galy-Lacaux, C., Xu, W., Neuman, J. A., Tang, Y. S., Sutton, M. A., Erisman, J. W. and Coheur, P.
 874 F.: Towards validation of ammonia (NH₃) measurements from the IASI satellite, Atmos.
 875 Meas. Tech., 8(3), 1575–1591, doi:10.5194/amt-8-1575-2015, 2015.
 876 Van Damme, M., Whitburn, S., Clarisse, L., Clerbaux, C., Hurtmans, D. and Coheur, P. F.:
 877 Version 2 of the IASI NH₃ neural network retrieval algorithm: Near-real-time and
 878 reanalysed datasets, Atmos. Meas. Tech., 10(12), 4905–4914, doi:10.5194/amt-10-4905-
 879 2017, 2017.
 880 Van Damme, M., Clarisse, L., Whitburn, S., Hadji-Lazaro, J., Hurtmans, D., Clerbaux, C. and
 881 Coheur, P.: Industrial and agricultural ammonia point sources exposed, Nature, 564, 99–
 882 103, 2018.
 883 Van Damme, M., Clarisse, L., Franco, B., Sutton, M. A., Erisman, J. W., Wichink Kruit, R., van
 884 Zanten, M., Whitburn, S., Hadji-Lazaro, J., Hurtmans, D., Clerbaux, C. and Coheur, P.-F.:
 885 Global, regional and national trends of atmospheric ammonia derived from a decadal
 886 (2008-2018) satellite record, Environ. Res. Lett., 2021.
 887 Dammers, E., Palm, M., Van Damme, M., Vigouroux, C., Smale, D., Conway, S., Toon, G. C.,
 888 Jones, N., Nussbaumer, E., Warneke, T., Petri, C., Clarisse, L., Clerbaux, C., Hermans, C.,
 889 Lutsch, E., Strong, K., Hannigan, J. W., Nakajima, H., Morino, I., Herrera, B., Stremme, W.,
 890 Grutter, M., Schaap, M., Kruit, R. J. W., Notholt, J., Coheur, P. F. and Erisman, J. W.: An
 891 evaluation of IASI-NH₃ with ground-based Fourier transform infrared spectroscopy
 892 measurements, Atmos. Chem. Phys., 16(16), 10351–10368, doi:10.5194/acp-16-10351-
 893 2016, 2016.
 894 Denier Van Der Gon, H. and Bleeker, A.: Indirect N₂O emission due to atmospheric N
 895 deposition for the Netherlands, Atmos. Environ., 39(32), 5827–5838,

doi:10.1016/j.atmosenv.2005.06.019, 2005.

Dobson, J. E., Bright, E. A., Coleman, P. R., Durfee, R. C. and Worley, B. A.: A global population database for estimating populations at risk, *Photogramm. Eng. Remote Sens.*, 66(7), 849–857 [online] Available from: In Book..., 2000.

Doumbia, E. H. T., Liousse, C., Keita, S., Granier, L., Granier, C., Elvidge, C. D., Elguindi, N. and Law, K.: Flaring emissions in Africa: Distribution, evolution and comparison with current inventories, *Atmos. Environ.*, 199(November 2018), 423–434, doi:10.1016/j.atmosenv.2018.11.006, 2019.

Elrys, A. S., Abdel-Fattah, M. K., Raza, S., Chen, Z. and Zhou, J.: Spatial trends in the nitrogen budget of the African agro-food system over the past five decades, *Environ. Res. Lett.*, 14(12), doi:10.1088/1748-9326/ab5d9e, 2019.

European Commission Joint Research Centre (JRC)/Netherlands Environmental Assessment Agency (PBL): Emission Database for Global Atmospheric Research (EDGAR), release version 4.3.1, 2016.

Fan, Y. and van den Dool, H.: A global monthly land surface air temperature analysis for 1948-present, *J. Geophys. Res. Atmos.*, 113(1), D01103, doi:10.1029/2007JD008470, 2008.

FAO: FAO Statistics Database, FAOSTAT Stat. Database [online] Available from: <http://www.fao.org/faostat/en/> (Accessed 1 January 2019), 2020.

Friedl, M. A., McIver, D. K., Hodges, J. C. F., Zhang, X. Y., Muchoney, D., Strahler, A. H., Woodcock, C. E., Gopal, S., Schneider, A., Cooper, A., Baccini, A., Gao, F. and Schaaf, C.: Global land cover mapping from MODIS: Algorithms and early results, *Remote Sens. Environ.*, 83(1–2), 287–302, doi:10.1016/S0034-4257(02)00078-0, 2002.

Galy-Lacaux, C. and Delon, C.: Nitrogen emission and deposition budget in West and Central Africa, *Environ. Res. Lett.*, 9(12), doi:10.1088/1748-9326/9/12/125002, 2014.

Gbadegesin, A. and Olusesi, B. B.: Effects of land clearing methods on soil physical and hydrological properties in southwestern Nigeria, *Environmentalist*, 14(4), 297–303 [online] Available from: <http://www.scopus.com/inward/record.url?eid=2-s2.0-0022858519&partnerID=40&md5=3051b1dd91ff2990e37fe7466872923e>, 1994.

George, M., Clerbaux, C., Hurtmans, D., Turquety, S., Coheur, P. F., Pommier, M., Hadji-Lazaro, J., Edwards, D. P., Worden, H., Luo, M., Rinsland, C. and McMillan, W.: Carbon monoxide distributions from the IASI/METOP mission: Evaluation with other space-borne

927 remote sensors, *Atmos. Chem. Phys.*, 9(21), 8317–8330, doi:10.5194/acp-9-8317-2009,
 928 2009.
 929 Giglio, L., Boschetti, L., Roy, D. P., Humber, M. L. and Justice, C. O.: The Collection 6 MODIS
 930 burned area mapping algorithm and product, *Remote Sens. Environ.*, 217, 72–85,
 931 doi:10.1016/j.rse.2018.08.005, 2018.
 932 Global Internal Displacement Monitoring Centre: Global Internal Displacement Database,
 933 [online] Available from: [https://www.internal-displacement.org/database/displacement-](https://www.internal-displacement.org/database/displacement-data)
 934 [data](https://www.internal-displacement.org/database/displacement-data), 2020.
 935 Goode, J. G., Yokelson, R. J., Susott, R. A. and Ward, D. E.: Trace gas emissions from
 936 laboratory biomass fires measured by open-path Fourier transform infrared spectroscopy;
 937 *J. Chem. Inf. Model.*, 104(D17), 21237–21245, 1999.
 938 Guo, X., Clarisse, L., Wang, R., Van Damme, M., Whitburn, S., Coheur, P., Clerbaux, C., Franco,
 939 B., Pan, D., Golston, L. M., Wendt, L., Sun, K., Tao, L., Miller, D., Mikoviny, T., Müller, M.,
 940 Wisthaler, A., Tevlin, A. G., Murphy, J. G., Nowak, J. B., Roscioli, J. R., Volkamer, R., Kille, N.,
 941 Neuman, J. A., Eilerman, S. J., Crawford, J. H., Yacovitch, T. I., Barrick, J. D., Scarino, A. J. and
 942 Zondlo, M. A.: Validation of IASI satellite ammonia observations at the pixel scale using in-
 943 situ vertical profiles, *J. Geophys. Res. Atmos.*, 126, e2020JD033475,
 944 doi:10.1029/2020jd033475, 2021.
 945 Hazell, P. and Wood, S.: Drivers of change in global agriculture., *Philos. Trans. R. Soc. Lond.*
 946 *B. Biol. Sci.*, 363(1491), 495–515, doi:10.1098/rstb.2007.2166, 2008.
 947 Hickman, Jonathan, E., Andela, N., Galy-Lacaux, C., Ossohou, M., Dammers, E., Van Damme,
 948 M., Clarisse, L., Tsigaridis, K. and Bauer, S. E.: Continental and ecoregion-specific drivers of
 949 atmospheric NO₂ and NH₃ seasonality over Africa revealed by satellite observations,
 950 *Global Biogeochem. Cycles*, *in review*,
 951 Hickman, J. E., Dammers, E., Galy-Lacaux, C. and Van Der Werf, G. R.: Satellite evidence of
 952 substantial rain-induced soil emissions of ammonia across the Sahel, *Atmos. Chem. Phys.*,
 953 18(22), 16713–16727, doi:10.5194/acp-18-16713-2018, 2018.
 954 Hickman, J. E., Andela, N., Tsigaridis, K., Galy-Lacaux, C., Ossohou, M. and Bauer, S. E.:
 955 Reductions in NO₂ burden over north equatorial Africa from decline in biomass burning in
 956 spite of growing fossil fuel use, 2005 to 2017, *Proc. Natl. Acad. Sci.*, 118(7), e2002579118,
 957 doi:10.1073/pnas.2002579118, 2021.

Deleted: n.d.

959 Huffman, G. J., Adler, R. F., Bolvin, D. T., Gu, G., Nelkin, E. J., Bowman, K. P., Hong, Y., Stocker,
 960 E. F. and Wolff, D. B.: The TRMM Multisatellite Precipitation Analysis (TMPA): Quasi-Global,
 961 Multiyear, Combined-Sensor Precipitation Estimates at Fine Scales, *J. Hydrometeorol.*, 8(1),
 962 38–55, doi:10.1175/jhm560.1, 2007.
 963 Hurtmans, D., Coheur, P. F., Wespes, C., Clarisse, L., Scharf, O., Clerbaux, C., Hadji-Lazaro, J.,
 964 George, M. and Turquety, S.: FORLI radiative transfer and retrieval code for IASI, *J. Quant.*
 965 *Spectrosc. Radiat. Transf.*, 113(11), 1391–1408, doi:10.1016/j.jqsrt.2012.02.036, 2012.
 966 Idris, I.: Livestock and conflict in South Sudan - K4D Helpdesk Report 484, Brighton.
 967 [online] Available from:
 968 https://assets.publishing.service.gov.uk/media/5c6abdec40f0b61a22792fd5/484_Livestock_and_Conflict_in_South_Sudan.pdf, 2018.
 969
 970 Kanter, D. R.: Nitrogen pollution: a key building block for addressing climate change, *Clim.*
 971 *Change*, 147(1–2), 11–21, doi:10.1007/s10584-017-2126-6, 2018.
 972 Kerzenmacher, T., Dils, B., Kumps, N., Blumenstock, T., Clerbaux, C., Coheur, P. F., Demoulin,
 973 P., García, O., George, M., Griffith, D. W. T., Hase, F., Hadji-Lazaro, J., Hurtmans, D., Jones, N.,
 974 Mahieu, E., Notholt, J., Paton-Walsh, C., Raffalski, U., Ridder, T., Schneider, M., Servais, C. and
 975 De Mazière, M.: Validation of IASI FORLI carbon monoxide retrievals using FTIR data from
 976 NDACC, *Atmos. Meas. Tech.*, 5(11), 2751–2761, doi:10.5194/amt-5-2751-2012, 2012.
 977 Korontzi, S., McCarty, J., Loboda, T., Kumar, S. and Justice, C.: Global distribution of
 978 agricultural fires in croplands from 3 years of Moderate Resolution Imaging
 979 Spectroradiometer (MODIS) data, *Global Biogeochem. Cycles*, 20(2), GB2021,
 980 doi:10.1029/2005GB002529, 2006.
 981 Krupa, S. V.: Effects of atmospheric ammonia (NH₃) on terrestrial vegetation: A review,
 982 *Environ. Pollut.*, 124(2), 179–221, doi:10.1016/S0269-7491(02)00434-7, 2003.
 983 Lee, C., Martin, R. V., Van Donkelaar, A., Lee, H., Dickerson, R. R., Hains, J. C., Krotkov, N.,
 984 Richter, A., Vinnikov, K. and Schwab, J. J.: SO₂ emissions and lifetimes: Estimates from
 985 inverse modeling using in situ and global, space-based (SCIAMACHY and OMI)
 986 observations, *J. Geophys. Res. Atmos.*, 116(6), 1–13, doi:10.1029/2010JD014758, 2011.
 987 Lelieveld, J., Evans, J. S., Fnais, M., Giannadaki, D. and Pozzer, A.: The contribution of outdoor
 988 air pollution sources to premature mortality on a global scale, *Nature*, 525(7569), 367–371,
 989 doi:10.1038/nature15371, 2015.

990 Nicholson, S., Some, B., McCollum, J., Nelkin, E., Klotter, D., Berte, Y., Diallo, B., Gaye, I.,
 991 Kpabeba, G., Ndiaye, O., Noukpozounkou, J., Tanu, M., Thiam, A., Toure, A. and Traore, A.:
 992 Validation of TRMM and other rainfall estimates with a high-density gauge dataset for West
 993 Africa. Part II: Validation of TRMM rainfall products, *J. Appl. Meteorol.*, 42, 1355–1368,
 994 doi:Article, 2003.
 995 Ossohou, M., Galy-Lacaux, C., Yoboué, V., Hickman, J. E., Gardrat, E., Adon, M., Darras, S.,
 996 Laouali, D., Akpo, A., Ouaf, M., Diop, B. and Opepa, C.: Trends and seasonal variability of
 997 atmospheric NO₂ and HNO₃ concentrations across three major African biomes inferred
 998 from long-term series of ground-based and satellite measurements, *Atmos. Environ.*, 207,
 999 148–166, 2019.
 1000 Pamela A. Matson, McDowell, W. H., Townsend, A. R. and Vitousek, P. M.: The globalization
 1001 of N deposition: ecosystem consequences in tropical environments, *Biogeochemistry*, 46,
 1002 67–83 [online] Available from: [http://academic.engr.arizona.edu/HWR/Brooks/GC572-](http://academic.engr.arizona.edu/HWR/Brooks/GC572-2004/readings/matson.pdf)
 1003 2004/readings/matson.pdf, 1999.
 1004 Pommier, M., Law, K. S., Clerbaux, C., Turquety, S., Hurtmans, D., Hadji-Lazaro, J., Coheur, P.
 1005 F., Schlager, H., Ancellet, G., Paris, J. D., Nédélec, P., Diskin, G. S., Podolske, J. R., Holloway, J. S.
 1006 and Bernath, P.: IASI carbon monoxide validation over the Arctic during POLARCAT spring
 1007 and summer campaigns, *Atmos. Chem. Phys.*, 10(21), 10655–10678, doi:10.5194/acp-10-
 1008 10655-2010, 2010.
 1009 Pope, A., Burnett, R., Thun, M., EE, C., D, K., I, K. and GD, T.: Long-term Exposure to Fine
 1010 Particulate Air Pollution, *J. Am. Med. Assoc.*, 287(9), 1132–1141,
 1011 doi:10.1001/jama.287.9.1132, 2002.
 1012 Raleigh, C., Linke, A., Hegre, H. and Karlsen, J.: Introducing ACLED: An Armed Conflict
 1013 Location and Event Dataset: Special Data Feature, *J. Peace Res.*, 47(5), 651–660,
 1014 doi:<https://doi.org/10.1177/0022343310378914>, 2010.
 1015 Ramo, R., Roteta, E., Bistinas, I., van Wees, D., Bastarrika, A., Chuvieco, E. and van der Werf,
 1016 G. R.: African burned area and fire carbon emissions are strongly impacted by small fires
 1017 undetected by coarse resolution satellite data, *Proc. Natl. Acad. Sci. U. S. A.*, 118(9), 1–7,
 1018 doi:10.1073/pnas.2011160118, 2021.
 1019 Robinson, T. P., Wint, G. R. W., Conchedda, G., Van Boeckel, T. P., Ercoli, V., Palamara, E.,
 1020 Cinardi, G., D'Aietti, L., Hay, S. I. and Gilbert, M.: Mapping the Global Distribution of

1021 Livestock, PLoS One, 9(5), e96084, doi:10.1371/journal.pone.0096084, 2014.
 1022 Roteta, E., Bastarrika, A., Padilla, M., Storm, T. and Chuvieco, E.: Development of a Sentinel-2
 1023 burned area algorithm: Generation of a small fire database for sub-Saharan Africa, Remote
 1024 Sens. Environ., 222(November 2018), 1–17, doi:10.1016/j.rse.2018.12.011, 2019.
 1025 Rufino, M. C., Rowe, E. C., Delve, R. J. and Giller, K. E.: Nitrogen cycling efficiencies through
 1026 resource-poor African crop-livestock systems, Agric. Ecosyst. Environ., 112(4), 261–282,
 1027 doi:10.1016/j.agee.2005.08.028, 2006.
 1028 Sauvage, B., Gheusi, F., Thouret, V., Cammas, J. P., Duron, J., Escobar, J., Mari, C., Mascart, P.
 1029 and Pont, V.: Medium-range mid-tropospheric transport of ozone and precursors over
 1030 Africa: Two numerical case studies in dry and wet seasons, Atmos. Chem. Phys., 7(20),
 1031 5357–5370, doi:10.5194/acp-7-5357-2007, 2007.
 1032 Stevens, C. J., David, T. I. and Storkey, J.: Atmospheric nitrogen deposition in terrestrial
 1033 ecosystems: Its impact on plant communities and consequences across trophic levels,
 1034 Funct. Ecol., 32(7), 1757–1769, doi:10.1111/1365-2435.13063, 2018.
 1035 Sutton, M. A., Reis, S., Riddick, S. N., Dragosits, U., Nemitz, E., Theobald, M. R., Tang, Y. S.,
 1036 Braban, C. F., Vieno, M., Dore, A. J., Mitchell, R. F., Wanless, S., Daunt, F., Fowler, D., Blackall,
 1037 T. D., Milford, C., Flechard, C. R., Loubet, B., Massad, R., Cellier, P., Personne, E., Coheur, P. F.,
 1038 Clarisse, L., Van Damme, M., Ngadi, Y., Clerbaux, C., Skøth, C. A., Geels, C., Hertel, O., Wichink
 1039 Kruit, R. J., Pinder, R. W., Bash, J. O., Walker, J. T., Simpson, D., Horváth, L., Misselbrook, T. H.,
 1040 Bleeker, A., Dentener, F. and de Vries, W.: Towards a climate-dependent paradigm of
 1041 ammonia emission and deposition, Philos. Trans. R. Soc. B Biol. Sci., 368(1621), 20130166–
 1042 20130166, doi:10.1098/rstb.2013.0166, 2013.
 1043 Tian, D. and Niu, S.: A global analysis of soil acidification caused by nitrogen addition,
 1044 Environ. Res. Lett., 10(2), 024019, doi:10.1088/1748-9326/10/2/024019, 2015.
 1045 USDA Agricultural Air Quality Task Force: Ammonia Emissions : What To Know Before You
 1046 Regulate, Washington, DC. [online] Available from:
 1047 <http://www.nrcs.usda.gov/wps/portal/nrcs/detail/national/air/taskforce/?cid=stelprdb1>
 1048 268645, 2014.
 1049 Vitousek, P., Naylor, R., Crews, T., David, M., Drinkwater, L., Holland, E., Johnes, P.,
 1050 Katzenberger, J., Martinelli, L. A., Matson, P. A., Nziguheba, G., Ojima, D., Palm, C. A.,
 1051 Robertson, G., Sanchez, P., Townsend, A. and Zhang, F.: Nutrient Imbalances in Agricultural

1052 Development, *Science* (80-), 324, 1519–1520, 2009.

1053 Di Vittorio, C. A. and Georgakakos, A. P.: Land cover classification and wetland inundation

1054 mapping using MODIS, *Remote Sens. Environ.*, 204(May 2017), 1–17,

1055 doi:10.1016/j.rse.2017.11.001, 2018.

1056 Vrieling, A., de Beurs, K. M. and Brown, M. E.: Variability of African farming systems from

1057 phenological analysis of NDVI time series, *Clim. Change*, 109(3–4), 455–477,

1058 doi:10.1007/s10584-011-0049-1, 2011.

1059 De Wachter, E., Barret, B., Le Flochmoën, E., Pavelin, E., Matricardi, M., Clerbaux, C., Hadji-

1060 Lazaro, J., George, M., Hurtmans, D., Coheur, P. F., Nedelec, P. and Cammas, J. P.: Retrieval of

1061 MetOp-A/IASI CO profiles and validation with MOZAIC data, *Atmos. Meas. Tech.*, 5(11),

1062 2843–2857, doi:10.5194/amt-5-2843-2012, 2012.

1063 Warner, J. X., Dickerson, R. R., Wei, Z., Strow, L. L., Wang, Y. and Liang, Q.: Increased

1064 atmospheric ammonia over the world’s major agricultural areas detected from space,

1065 *Geophys. Res. Lett.*, 44(6), 2875–2884, doi:10.1002/2016GL072305, 2017.

1066 Whitburn, S., Van Damme, M., Kaiser, J. W., Van Der Werf, G. R., Turquety, S., Hurtmans, D.,

1067 Clarisse, L., Clerbaux, C. and Coheur, P. F.: Ammonia emissions in tropical biomass burning

1068 regions: Comparison between satellite-derived emissions and bottom-up fire inventories,

1069 *Atmos. Environ.*, 121, 42–54, doi:10.1016/j.atmosenv.2015.03.015, 2015.

1070 World Bank: World Bank Open Data, World Bank Open Data [online] Available from:

1071 <https://www.data.worldbank.org> (Accessed 2 February 2019).

1072 Yegbemey, R. N., Kabir, H., Awoye, O. H. R., Yabi, J. A. and Paraíso, A. A.: Managing the

1073 agricultural calendar as coping mechanism to climate variability: A case study of maize

1074 farming in northern Benin, West Africa, *Clim. Risk Manag.*, 3, 13–23,

1075 doi:10.1016/j.crm.2014.04.001, 2014.

1076 Yokelson, R. J., Christian, T. J., Karl, T. G. and Guenther, A.: The tropical forest and fire

1077 emissions experiment: laboratory fire measurements and synthesis of campaign, *Rev. Int.*

1078 *Acupunt.*, 8, 3509–3527, doi:10.1016/s1887-8369(09)71579-0, 2008.

1079 Zheng, B., Chevallier, F., Ciais, P., Yin, Y. and Wang, Y.: On the Role of the Flaming to

1080 Smoldering Transition in the Seasonal Cycle of African Fire Emissions, *Geophys. Res. Lett.*,

1081 45(21), 11,998–12,007, doi:10.1029/2018GL079092, 2018.

1082

Deleted: , n.d.

Page 17: [1] Deleted Hickman, Jonathan E. (GISS-611.0)[SciSpace LLC] 4/9/21 10:49:00 AM

▼

Page 17: [1] Deleted Hickman, Jonathan E. (GISS-611.0)[SciSpace LLC] 4/9/21 10:49:00 AM

▼

Page 17: [1] Deleted Hickman, Jonathan E. (GISS-611.0)[SciSpace LLC] 4/9/21 10:49:00 AM

▼

Page 17: [2] Deleted Hickman, Jonathan E. (GISS-611.0)[SciSpace LLC] 4/14/21 11:47:00 AM

▼

Page 17: [2] Deleted Hickman, Jonathan E. (GISS-611.0)[SciSpace LLC] 4/14/21 11:47:00 AM

▼

Page 17: [2] Deleted Hickman, Jonathan E. (GISS-611.0)[SciSpace LLC] 4/14/21 11:47:00 AM

▼

Page 17: [2] Deleted Hickman, Jonathan E. (GISS-611.0)[SciSpace LLC] 4/14/21 11:47:00 AM

▼

Page 17: [3] Deleted Hickman, Jonathan E. (GISS-611.0)[SciSpace LLC] 4/9/21 10:50:00 AM

▼

